PHYSICAL REVIEW B **90**, 041112(R) (2014)

α-$RuCl_3$: A spin-orbit assisted Mott insulator on a honeycomb lattice

K. W. Plumb,[1] J. P. Clancy,[1] L. J. Sandilands,[1] V. Vijay Shankar,[1] Y. F. Hu,[2] K. S. Burch,[1,3]
Hae-Young Kee,[1,4] and Young-June Kim[1,*]

[1]*Department of Physics and Center for Quantum Materials, University of Toronto, 60 St. George St., Toronto, Ontario, Canada M5S 1A7*
[2]*Canadian Light Source, Saskatoon, Saskatchewan, Canada S7N 0X4*
[3]*Department of Physics, Boston College, Chestnut Hill, Massachusetts 02467, USA*
[4]*Canadian Institute for Advanced Research, Toronto, Ontario, Canada M5G 1Z8*

(Received 18 March 2014; revised manuscript received 30 June 2014; published 29 July 2014)

We examine the role of spin-orbit coupling in the electronic structure of α-$RuCl_3$, in which Ru ions in $4d^5$ configuration form a honeycomb lattice. Our x-ray absorption spectroscopy measurements at the Ru L edges exhibit distinct spectral features associated with the presence of substantial spin-orbit coupling, as well as an anomalously large branching ratio. Furthermore the measured optical spectra can be described very well with first-principles electronic structure calculations obtained by taking into account both spin-orbit coupling and electron correlations. We propose that α-$RuCl_3$ is a spin-orbit assisted Mott insulator, and that the bond-dependent Kitaev interaction may be important for understanding magnetism of this compound.

DOI: 10.1103/PhysRevB.90.041112 PACS number(s): 75.10.Jm, 71.20.Be, 71.70.Ej, 78.70.Dm

Novel electronic ground states can often result from the interplay of many competing energy scales. In magnetic materials containing heavy transition metals such as iridium, the combination of electronic correlations and spin-orbit coupling (SOC) can give rise to exotic topological phases [1–11]. For example, when a $4d^5$ or $5d^5$ ion is subject to an octahedral crystal field environment, SOC mixes the wave functions of the triply degenerate t_{2g} electronic states and the low-energy magnetic degrees of freedom are described by spin-orbital mixed Kramers doublets, termed J_{eff} states [6,7,12]. One of many interesting consequences of J_{eff} states in real materials is the presence of an unusual bond-dependent exchange term called the Kitaev interaction. This bond-dependent magnetic interaction is fundamentally different from the usual isotropic or anisotropic Heisenberg interaction, since frustration is naturally present on a single site. This allows unconventional quantum ground states, such as spin liquids, to emerge even in the absence of geometrical frustration [1,7]. Such a bond-dependent interaction is an important ingredient for the quantum compass model, which is relevant in various physical contexts ranging from ultracold atomic gases to topological quantum computing [13].

Experimentally, current efforts are mostly directed towards studying the $5d$ A_2IrO_3 (A = Na or Li) compounds where IrO_6 octahedra share edges to form a honeycomb network [14–20]. The edge-sharing geometry suppresses isotropic Heisenberg interactions, while Kitaev interactions are believed to be substantial [6,7]. However, due to monoclinic and trigonal distortions, the applicability of the localized J_{eff} picture to these compounds is still controversial [21,22]. Materials with $4d$ electrons have not drawn much attention due to their smaller SOC compared to $5d$ systems. However, even if the absolute value of SOC in $4d$ systems is smaller than that of $5d$ elements, the J_{eff} state may still be realized as long as the t_{2g} states remain degenerate in the absence of SOC [23]. α-$RuCl_3$ is an insulating $4d$ transition-metal halide with honeycomb layers composed of nearly ideal edge-sharing $RuCl_6$ octahedra, and therefore an excellent candidate material in which bond-dependent Kitaev interactions may be found. In addition, single crystal samples are extremely micaceous, similar to graphite, and can potentially be used to produce a truly two-dimensional quantum magnet. While earlier transport measurements have implicated α-$RuCl_3$ to be a conventional semiconductor [24], subsequent spectroscopic investigations suggest that it may be a Mott insulator [25]. However, a systematic examination of the role of SOC in the electronic structure of α-$RuCl_3$ has not been conducted until now.

In this Rapid Communication, we show that the insulating state in α-$RuCl_3$ arises from the combined effects of electronic correlations and strong SOC. Our x-ray absorption spectroscopy (XAS) data directly indicates that substantial SOC of Ru is present in α-$RuCl_3$. In order to probe the detailed electronic structure, we have carried out optical spectroscopy measurements. The origins of the optical gap in α-$RuCl_3$ are elucidated by our band structure calculations. We find that while strong electronic correlations are necessary to describe this material, SOC is essential to account for the magnitude of the optical gap. Taken as a whole, our results indicate that α-$RuCl_3$ is best described as a spin-orbit assisted Mott insulator and strong SOC effects must be considered to understand this material.

The crystal structure of α-$RuCl_3$ is shown in Fig. 1. Edge-sharing $RuCl_6$ octahedra form a honeycomb network in the a-b plane and the weakly coupled honeycomb layers are stacked along the c direction to form a $CrCl_3$-type structure $P3_112$ [27]. As shown in Fig. 1(c), the Cl-Ru-Cl angles are all within 1° of 90° and the Ru-Cl bond lengths are within 0.3% of one another. Thus, the $RuCl_6$ octahedron in this compound is very close to ideal. In fact, the absence of appreciable electric quadrupole interactions from the ^{99}Ru Mössbauer spectroscopy study was interpreted to result from the highly symmetric octahedral configuration of the ligand Cl ions [28]. This structural detail is quite important since such an ideal octahedral environment will leave the t_{2g} states degenerate in the absence of SOC. In contrast, Na_2IrO_3 has an O-Ir-O bond angle of about 85° [17,18]. Another important structural difference between Na_2IrO_3 and α-$RuCl_3$ is the lack

*yjkim@physics.utoronto.ca

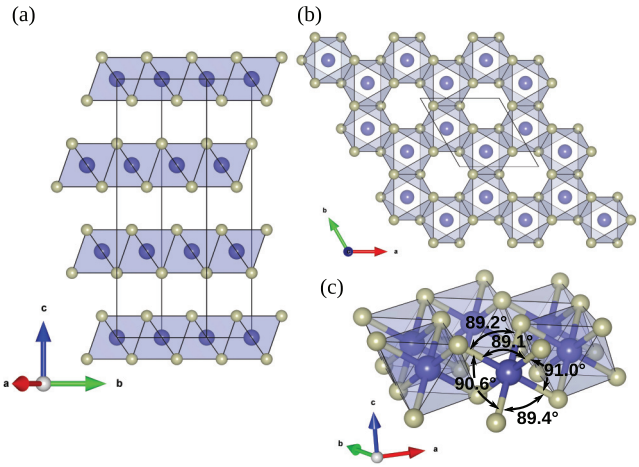

FIG. 1. (Color online) (a) The crystal structure of α-$RuCl_3$, exhibiting lamellar nature of the unit cell. (b) Individual honeycomb layers are formed by edge-sharing $RuCl_6$ octahedra (Ru in blue, Cl in gray). (c) Detailed view of $RuCl_6$ octahedra showing bond angles. All the figures were produced with VESTA [26].

of intervening Na atoms between the honeycomb layers in the latter compound, such that α-$RuCl_3$ is closer to an ideal two-dimensional system.

Single crystal samples of α-$RuCl_3$ were prepared by vacuum sublimation from commercial $RuCl_3$ powder. The dielectric function $\hat{\epsilon}(\omega) = \epsilon_1(\omega) + \epsilon_2(\omega)$ of $RuCl_3$ was measured from 0.1 to 6 eV; for the range 0.9–6 eV, $\hat{\epsilon}(\omega)$ was determined using spectroscopic ellipsometry. From 0.1 to 1.2 eV, we measured the transmittance through a thin $RuCl_3$ sample and extracted $\hat{\epsilon}(\omega)$ using a standard model for the transmittance of a plate sample [29]. X-ray absorption spectroscopy measurements were performed using the soft x-ray microcharacterization beamline (SXRMB) at the Canadian Light Source. Measurements were carried out at the Ru L_3 ($2p_{3/2} \rightarrow 4d$) and L_2 ($2p_{1/2} \rightarrow 4d$) absorption edges [30].

Physical properties of α-$RuCl_3$ have been extensively investigated. The magnetic susceptibility of α-$RuCl_3$ shows a sharp cusp around 13–15 K, which was attributed to antiferromagnetic ordering [31]; and a Curie-Weiss fit yields an effective local moment of about $2.2\mu_B$ and ferromagnetic Curie-Weiss temperatures of 23–40 K [28,31]. The effective magnetic moment is much larger than the spin-only value of $1.73\mu_B$ for the low spin ($S = 1/2$) state of Ru^{3+}, indicating a significant orbital contribution to total moment. Based on these observations, it was suggested that the nearest-neighbor interaction within the honeycomb plane is ferromagnetic and that these planes are weakly coupled with an antiferromagnetic interaction. However, powder neutron diffraction failed to observe magnetic Bragg peaks of (003) type, which are expected from the predicted simple magnetic structure [31]. Although several spectroscopic and transport investigations have been carried out to study the electronic structure of α-$RuCl_3$ [24,25,32,33], the role of SOC was not explored in detail in these earlier studies.

The importance of SOC in the electronic structure of α-$RuCl_3$ can be revealed through XAS measurements. The x-ray absorption spectra obtained at the Ru L_2 and L_3 edges

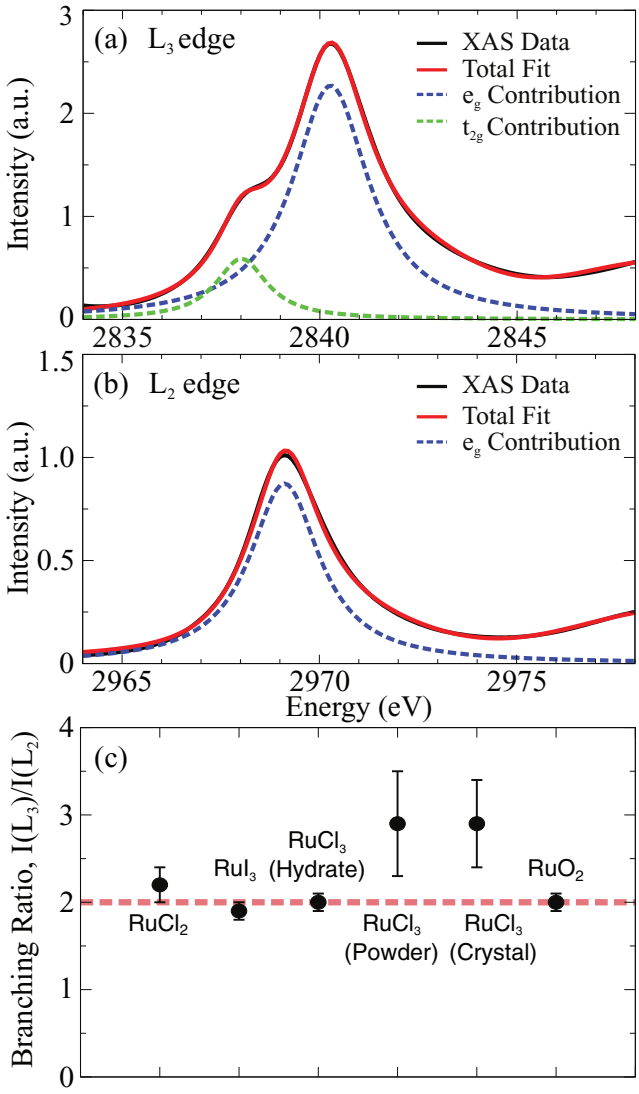

FIG. 2. (Color online) (a) X-ray absorption near-edge spectra of $RuCl_3$ measured at the Ru L_3 edge. The black solid line is the experimental data, and the red solid line is a fit function that includes two Lorentzian peaks associated with t_{2g} and e_g states and an arctan function describing the edge jump. (b) Same spectra showing the energy range of the Ru L_2 edge. The scale is exactly half of the one shown in (a), emphasizing the departure from the statistical branching ratio of 2. (c) Comparison of the branching ratio with various Ru standard compounds, ranging from Ru^{2+} ($RuCl_2$), Ru^{3+} (RuI_3), to Ru^{4+} (RuO_2). Note that $RuCl_3$ (hydrate) has a structure different from α-$RuCl_3$ studied here.

are shown in Fig. 2. Two peaks are observed for the L_3 edge data shown in Fig. 2(a), corresponding to exciting $2p_{3/2}$ core electrons into empty t_{2g} and e_g states. The intensity ratio between these two features is related to the fact that there is only one empty t_{2g} state available for the transition compared to four empty e_g states. A quantitative description of the intensity and the peak splitting requires ligand field multiplet calculations and is beyond the scope of this Rapid Communication. Here we instead focus on the different line shapes observed near the Ru L_2edge compared to that of the L_3

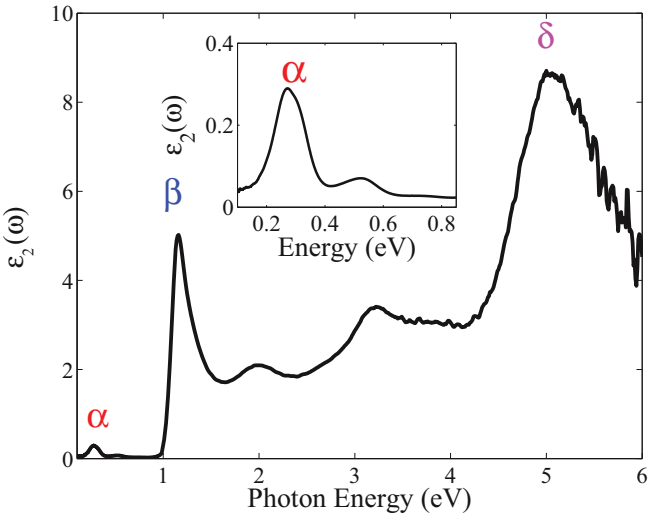

FIG. 3. (Color online) Imaginary component of the dielectric function $\epsilon_2(\omega)$ of $RuCl_3$ measured at 295 K. The spectrum displays three types of excitations: transitions between t_{2g} bands in the region from 0 to 1 eV; $t_{2g} \rightarrow e_g$ transitions spanning 1 to 4 eV; and charge transfer excitations in the range of 4 to 6 eV. The peak locations and intensities, as well as the optical gap size, are in good agreement with the LDA + SOC + U band structure. The transitions corresponding to the features labeled α, β, and δ are shown in Fig. 4(a). Inset: region around feature α is magnified.

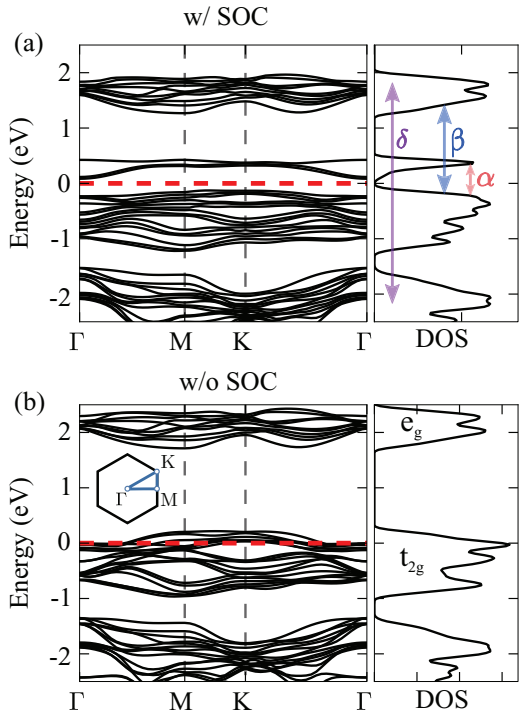

FIG. 4. (Color online) (a) LDA + U + SOC band structure and DOS of α-$RuCl_3$ along in plane high symmetry points of the BZ ($k_z = 0$) with $U = 1.5$ eV and $J_H = 0.3$ eV. The top panel is obtained with SOC and the bottom panel is without the SOC. Optical transitions are denoted with arrows and labels using the same notation as in Fig. 3.

edge. In particular, the lower-energy shoulder corresponding to the transition to the t_{2g} state is absent for the L_2 edge data. The different line shapes arise from SOC in the 4d electronic states. At the L_2 ($2p_{1/2}$) edge, the atomic dipole transition $2p_{1/2} \rightarrow 4d_{3/2}$ is allowed, while the J selection rule forbids the $2p_{1/2} \rightarrow 4d_{5/2}$ transition. This is different from the L_3 edge case, in which both $2p_{3/2} \rightarrow 4d_{3/2}$ and $2p_{3/2} \rightarrow 4d_{5/2}$ transitions are dipole allowed. The absence of the L_2 peak indicates that the empty t_{2g} state takes on $J = 5/2$ character; a result of significant SOC effects. The fact that the line shape depends crucially on the 4d SOC was first noted by Sham *et al.* in their study of $Ru(NH_3)_6Cl_6$ [34], and later confirmed quantitatively in the multiplet calculation carried out by de Groot *et al.* [35].

Another quantity often used to illustrate the strength of SOC is the so-called branching ratio, defined as the main peak ("white line") intensity ratio between the L_3 and L_2 absorption features. Typically, this value is about 2. However, when the d-electron SOC is significant, anomalously larger values have been observed; for example, many iridate compounds show large branching ratios [36]. If we take both peaks in the L_3 edge data into account, the branching ratio of α-$RuCl_3$ is also quite large: 3.0 ± 0.5. In Fig. 2(c), the observed branching ratios for several Ru-containing compounds are compared. Clearly α-$RuCl_3$ exhibits an anomalously large value. Thus, both the line shape and the branching ratio indicate that the SOC in α-$RuCl_3$ is substantial.

In order to get a full picture of the low-energy electronic structure of α-$RuCl_3$, we have conducted optical spectroscopy measurements. In Fig. 3 we show the measured imaginary component of the dielectric function, $\epsilon_2(\omega)$. We find no evidence of free carrier absorption which confirms the insulating character of $RuCl_3$. The spectrum can be divided into three regions: (i) a series of weak transitions in the range 0.1–1 eV, (ii) three stronger features located near 1.2, 2, and 3.2 eV, and (iii) an intense band centered near 5 eV, in agreement with previous reports [24,32]. Representative features are labeled α, β, and δ as shown in Fig. 3 to facilitate a comparison with the band structure calculation. The inset of Fig. 3 shows the region around feature α in more detail.

The role of electronic correlations and SOC in generating the optical spectra can be understood from our electronic structure calculations. The band structure and total density of states (DOS) for α-$RuCl_3$ were obtained by performing first-principles calculations including SOC and are plotted in Fig. 4 [37]. In Fig. 4(a), we show the band structure and DOS obtained with Hubbard $U = 1.5$ eV and Hund's coupling $J_H = 0.3$ eV in the presence of SOC. The strength of electron correlation $U = 1.5$ eV was determined by comparing the direct charge gap with the measured optical gap. The Hund's coupling was chosen to be about 20% of U, which is typical for 3d or 4d transition-metal compounds. On the other hand, Fig. 4(b) presents the case with the same U and J_H strengths as in Fig. 4(a), but in the absence of the SOC. For both cases, one can see clearly the t_{2g} and $e_g$crystal field splitting due to the octahedral environment. However, the key difference is that Fig. 4(a) shows an insulating phase with an unambiguous charge gap, while the band structure is metallic when the SOC is absent as shown in Fig. 4(b). To obtain an insulating state without SOC, a Hubbard U value greater than 2.5 eV is required. This in turn produces a much larger value for the

charge gap which is constrained by the measured optical gap. Therefore, a reasonable description of the insulating phase in α-$RuCl_3$ is only possible through the combination of SOC and electron correlation.

Our LDA + U + SOC band structure also agrees well with the optical spectra at higher energies. The α peak, together with the other weak features below 1 eV, can be understood as transitions between t_{2g} bands. We assign the β feature to the lowest energetically allowed transition between the t_{2g} and e_g bands as represented by the arrow in Fig. 4(a); the features at 2 and 3.2 eV also involve this combination of initial and final states. Finally, we interpret the strong peak near 5 eV (feature δ) as due to transitions from the band 2 eV below the Fermi level to the e_g bands. Indeed, our density functional theory calculations suggest the band at -2 eV has an increased Cl p content, meaning the δ transition has a charge transfer character. Overall, our optical spectroscopy measurements and electronic structure calculations agree well, and thus identify α-$RuCl_3$ as a spin-orbit assisted Mott insulator.

The perceived similarities of both the crystal and electronic structure between Na_2IrO_3 and α-$RuCl_3$ naturally raises questions regarding the relevance of the Kitaev model to α-$RuCl_3$. As mentioned earlier, Na_2IrO_3 is under intense scrutiny due to the possibility of realizing a Kitaev spin liquid phase [1,5,7,10,14–20,38,39]. However, the trigonal distortion present in Na_2IrO_3 brings the atomic basis of the spin-orbit coupled $J_{\text{eff}} = 1/2$ states into question [21,22]. Furthermore, Na atoms may promote non-negligible further neighbor exchange terms additional to the nearest-neighbor terms [39,40]. α-$RuCl_3$ is free from such complexity as it is close to the ideal two-dimensional honeycomb lattice. Even though the atomic SOC is weaker, the ratio of the SOC and the electronic bandwidth is only slightly smaller than in Na_2IrO_3 because both are reduced in α-$RuCl_3$ compared to iridates. Indeed we find the bandwidth of α-$RuCl_3$ to be about half of that in Na_2IrO_3, while the SOC is smaller by a factor of $\sim$3. More detailed electronic structure calculations have found that the bands near the Fermi level in α-$RuCl_3$ are mostly composed of $J_{\text{eff}} = 1/2$ except in the region near the Γ point [41]; this situation is similar to perovskite iridates [42,43]. Another important difference between Na_2IrO_3 and α-$RuCl_3$ is the large size of Cl anions which expands the lattice; the Ru-Ru distance is about 10% larger than the Ir-Ir distance in Na_2IrO_3. As a result, the direct hopping between the Ru t_{2g} orbitals is suppressed, and indirect hopping through Cl, which gives rise to a Kitaev interaction, is the most dominant hopping process in α-$RuCl_3$. Then a microscopic spin model relevant for α-$RuCl_3$ should be composed of both the nearest-neighbor Heisenberg and bond-dependent exchange terms denoted by Kitaev K and Γ [44–46].

In conclusion, we have carried out combined optical spectroscopy, electronic structure calculations, and x-ray absorption spectroscopy investigation of the role of spin-orbit coupling in α-$RuCl_3$. We find that both spin-orbit coupling and electron correlations are necessary to produce an electronic structure consistent with the observed optical gap of about 0.2 eV. In addition, the calculated electronic structure agrees with measured higher-energy optical transitions. Our x-ray absorption spectra clearly illustrate that spin-orbit coupling of the 4d electron system in this compound is significant. Thus spin-orbit coupling plays an essential role in the microscopic magnetic Hamiltonian, and α-$RuCl_3$ is likely to exhibit unconventional magnetic ordering arising from bond-dependent Kitaev interactions which could be investigated in future studies.

Research at the University of Toronto was supported by the NSERC, CFI, OMRI, and Canada Research Chair program. Computations were performed on the GPC supercomputer at the SciNet HPC Consortium [47]. SciNet is funded by the Canada Foundation for Innovation under the auspices of Compute Canada, the Government of Ontario, Ontario Research Fund—Research Excellence, and the University of Toronto. Research described in this paper was performed at the Canadian Light Source, which is funded by the Canada Foundation for Innovation, the Natural Sciences and Engineering Research Council of Canada, the National Research Council Canada, the Canadian Institutes of Health Research, the Government of Saskatchewan, Western Economic Diversification Canada, and the University of Saskatchewan.

[1] A. Kitaev, Ann. Phys. **321**, 2 (2006).
[2] X. Wan, A. M. Turner, A. Vishwanath, and S. Y. Savrasov, Phys. Rev. B **83**, 205101 (2011).
[3] Y. Okamoto, M. Nohara, H. Aruga-Katori, and H. Takagi, Phys. Rev. Lett. **99**, 137207 (2007).
[4] M. J. Lawler, A. Paramekanti, Y. B. Kim, and L. Balents, Phys. Rev. Lett. **101**, 197202 (2008).
[5] A. Shitade, H. Katsura, J. Kuneš, X.-L. Qi, S.-C. Zhang, and N. Nagaosa, Phys. Rev. Lett. **102**, 256403 (2009).
[6] G. Jackeli and G. Khaliullin, Phys. Rev. Lett. **102**, 017205 (2009).
[7] J. Chaloupka, G. Jackeli, and G. Khaliullin, Phys. Rev. Lett. **105**, 027204 (2010).
[8] D. Pesin and L. Balents, Nat. Phys. **6**, 376 (2010).
[9] W. Witczak-Krempa and Y. B. Kim, Phys. Rev. B **85**, 045124 (2012).
[10] J. Reuther, R. Thomale, and S. Trebst, Phys. Rev. B **84**, 100406 (2011).
[11] I. Kimchi and A. Vishwanath, Phys. Rev. B **89**, 014414 (2014).
[12] B. J. Kim, H. Jin, S. J. Moon, J.-Y. Kim, B.-G. Park, C. S. Leem, J. Yu, T. W. Noh, C. Kim, S.-J. Oh *et al.*, Phys. Rev. Lett. **101**, 076402 (2008).
[13] Z. Nussinov and J. van den Brink, arXiv:1303.5922.
[14] Y. Singh and P. Gegenwart, Phys. Rev. B **82**, 064412 (2010).
[15] X. Liu, T. Berlijn, W.-G. Yin, W. Ku, A. Tsvelik, Y.-J. Kim, H. Gretarsson, Y. Singh, P. Gegenwart, and J. P. Hill, Phys. Rev. B **83**, 220403 (2011).
[16] Y. Singh, S. Manni, J. Reuther, T. Berlijn, R. Thomale, W. Ku, S. Trebst, and P. Gegenwart, Phys. Rev. Lett. **108**, 127203 (2012).

[17] S. K. Choi, R. Coldea, A. N. Kolmogorov, T. Lancaster, I. I. Mazin, S. J. Blundell, P. G. Radaelli, Y. Singh, P. Gegenwart, K. R. Choi *et al.*, Phys. Rev. Lett. **108**, 127204 (2012).
[18] F. Ye, S. Chi, H. Cao, B. C. Chakoumakos, J. A. Fernandez-Baca, R. Custelcean, T. F. Qi, O. B. Korneta, and G. Cao, Phys. Rev. B **85**, 180403 (2012).
[19] R. Comin, G. Levy, B. Ludbrook, Z.-H. Zhu, C. N. Veenstra, J. A. Rosen, Y. Singh, P. Gegenwart, D. Stricker, J. N. Hancock *et al.*, Phys. Rev. Lett. **109**, 266406 (2012).
[20] H. Gretarsson, J. P. Clancy, X. Liu, J. P. Hill, E. Bozin, Y. Singh, S. Manni, P. Gegenwart, J. Kim, A. H. Said *et al.*, Phys. Rev. Lett. **110**, 076402 (2013).
[21] I. I. Mazin, H. O. Jeschke, K. Foyevtsova, R. Valentí, and D. I. Khomskii, Phys. Rev. Lett. **109**, 197201 (2012).
[22] K. Foyevtsova, Harald O. Jeschke, I. I. Mazin, D. I. Khomskii, and R. Valentí, Phys. Rev. B **88**, 035107 (2013).
[23] G. Chen, R. Pereira, and L. Balents, Phys. Rev. B **82**, 174440 (2010).
[24] L. Binotto, I. Pollini, and G. Spinolo, Phys. Status Solidi B **44**, 245 (1971).
[25] I. Pollini, Phys. Rev. B **53**, 12769 (1996).
[26] K. Momma and F. Izumi, J. Appl. Crystallogr. **44**, 1272 (2011).
[27] E. V. Stroganov and K. V. Ovchinnikov, Vestnik. Leningrad. Univ., Ser. Fiz. i Khim. **12**, 152 (1957).
[28] Y. Kobayashi, T. Okada, K. Asai, M. Katada, H. Sano, and F. Ambe, Inorg. Chem. **31**, 4570 (1992).
[29] A. Kuzmenko, *Reffit: Software to Fit Optical Spectra*, http://optics.unige.ch/alexey/reffit.html, 2014.
[30] See Supplemental Material at http://link.aps.org/supplemental/10.1103/PhysRevB.90.041112 and Refs. [48–50] therein for details of the experimental procedure.
[31] J. M. Fletcher, W. E. Gardner, A. C. Fox, and G. Topping, J. Chem. Soc. A 1038 (1967).
[32] G. Guizzetti, E. Reguzzoni, and I. Pollini, Phys. Lett. A **70**, 34 (1979).
[33] S. Rojas and G. Spinolo, Solid State Commun. **48**, 349 (1983).
[34] T. K. Sham, J. Am. Chem. Soc. **105**, 2269 (1983).
[35] F. M. F. de Groot, Z. W. Hu, M. F. Lopez, G. Kaindl, F. Guillot, and M. Tronc, J. Chem. Phys. **101**, 6570 (1994).
[36] J. P. Clancy, N. Chen, C. Y. Kim, W. F. Chen, K. W. Plumb, B. C. Jeon, T. W. Noh, and Y.-J. Kim, Phys. Rev. B **86**, 195131 (2012).
[37] See Supplemental Material at http://link.aps.org/supplemental/10.1103/PhysRevB.90.041112 and Refs. [51–54] for details of the calculation.
[38] S. Bhattacharjee, S.-S. Lee, and Y. B. Kim, New J. Phys. **14**, 073015 (2012).
[39] J. Chaloupka, G. Jackeli, and G. Khaliullin, Phys. Rev. Lett. **110**, 097204 (2013).
[40] I. Kimchi and Y.-Z. You, Phys. Rev. B **84**, 180407 (2011).
[41] V. Vijay Shankar and H.-Y. Kee (unpublished).
[42] J.-M. Carter and H.-Y. Kee, Phys. Rev. B **87**, 014433 (2013).
[43] J.-M. Carter, V. Shankar V., and H.-Y. Kee, Phys. Rev. B **88**, 035111 (2013).
[44] J. G. Rau, Eric Kin-Ho Lee, and H.-Y. Kee, Phys. Rev. Lett. **112**, 077204 (2014).
[45] Y. Yamaji, Y. Nomura, M. Kurita, R. Arita, and M. Imada, arXiv:1402.1030.
[46] V. M. Katukuri, S. Nishimoto, V. Yushankhai, A. Stoyanova, H. Kandpal, S. Choi, R. Coldea, I. Rousochatzakis, L. Hozoi, and J. van den Brink, New J. Phys. **16**, 013056 (2014).
[47] C. Loken, D. Gruner, L. Groer, R. Peltier, N. Bunn, M. Craig, T. Henriques, J. Dempsey, C.-H. Yu, J. Chen *et al.*, J. Phys.: Conf. Series **256**, 012026 (2010).
[48] P. Yu and M. Cardona, *Fundamentals of Semiconductors: Physics and Materials Properties* (Springer, New York, 2010).
[49] A. B. Kuzmenko, Rev. Sci. Instrum. **76**, 083108 (2005).
[50] B. Ravel and M. Newville, J. Synchrotron Radiat. **12**, 537 (2005).
[51] See http://elk.sourceforge.net.
[52] D. M. Ceperley and B. Alder, Phys. Rev. Lett. **45**, 566 (1980).
[53] J. P. Perdew and A. Zunger, Phys. Rev. B **23**, 5048 (1981).
[54] M. Czyżyk and G. Sawatzky, Phys. Rev. B **49**, 14211 (1994).